

Contact wear mechanisms of a dental composite with high filler content

V. S. NAGARAJAN *, B. J. HOCKEY, S. JAHANMIR
National Institute of Standards and Technology, Gaithersburg, MD 20899, USA
E-mail: sdid@nist.gov

V. P. THOMPSON
University of Medicine and Dentistry of New Jersey, Newark, NJ 07103, USA

The contact wear behavior of a dental ceramic composite containing 92 wt% silica glass and alumina filler particles in a polymeric resin matrix was examined. Because this composite is used for dental restorations, the tests were conducted under contact conditions that were relevant to those that exist in the mouth. Wear tests were conducted on a pin-on-disk tribometer with water as a lubricant. Results on wear volume as a function of load indicated two distinct regimes of wear. The wear volume increased slightly as the load was increased from 1 to 5 N. As the load was further increased to 10 N, the wear volume increased by one order of magnitude. At loads above 10 N (up to a maximum of 20 N), the wear volume was found to be independent of load. Examination of the wear tracks by SEM revealed that a surface film had formed on the wear tracks at all loads. Examination of these films by TEM showed that the films contained a mixture of small gamma-Al₂O₃ crystallites and glass particles. FTIR analysis of the adhered films indicated the presence of hydrated forms of silica and alumina, suggesting reaction of filler particles with water. Chemical analysis by ICP-MS of water samples collected after the wear tests confirmed the presence of Al and other elemental constituents of the filler particles. It is proposed that three simultaneous processes occur at the sliding contact: tribochemical reactions and film formation, dissolution of the reacted products, and mechanical removal of the film by microfracture. At low loads, wear occurs primarily by a tribochemical mechanism, i.e., formation and dissolution of the reaction products. At higher loads, wear occurs by a combination of tribochemical processes and mechanical detachment of the surface film. © 2000 Kluwer Academic Publishers

1. Introduction

Dental restorations, such as crowns, have traditionally been made out of pure metals or metal alloys, which often require ceramic porcelain coatings to obtain good esthetics [1, 2]. For the past two decades, efforts have been directed towards the development of ceramic [3–6] and composite [5, 7–10] restorations to match not only the chemical and mechanical properties of dental enamel, but its appearance as well. Unfilled methyl methacrylate resins were one of the first of this new class of restorative materials in dentistry, although use was confined to the anterior teeth [2]. In order to increase strength and hardness and to reduce polymerization shrinkage, tooth colored polymer resin matrix composites containing inorganic filler particles, such as glass or quartz, have been developed for dental restorations [5, 7, 8].

It has been reported that the mechanical properties of these composites are influenced by the filler concen-

tration, filler particle size, and polymerization shrinkage of the matrix resin [11, 12]. For example, Johnson *et al.* [11] studied the effect of filler content (from 0 to 44 wt%) on fracture toughness of resin composites. They found that, although the hardness was increased, the fracture toughness of the composites was reduced as the filler content was increased. In a related study, Htang *et al.* [12] found no effect on the fatigue resistance of a resin composite due to an increase in the filler content.

Wear behavior of filler-resin composites has been investigated under a variety of test conditions [7, 9, 13–16]. Resin composites undergo two types of wear in the oral environment, referred to as generalized wear and contact wear. Generalized wear is thought to be based upon three body wear caused by movement of food over the composite surface during mastication. Contact wear results from tooth to restorative material or restorative material to restorative material contacts.

* Present address: Lucent Technologies, Norcross, GA 30071, USA.

** Information on product names, manufacturers, and suppliers is included in this paper for clarity. This does not imply endorsement by the National Institute of Standards and Technology.

Early studies of dental composite resins have not made a distinction between the two types of wear because generalized wear was considered to be the primary wear mode. The complexity of the problem has led to a variety of test conditions and test methods [7, 9, 13–15]. In this paper, we concentrate on contact wear, which is also an important wear mode in dental composite resins.

Durand *et al.* [16] found that while small filler particles had no beneficial effect on wear, large filler particles reduced the wear of the matrix resin. Their results showed that wear resistance of the composite was improved as the volume fraction of large filler particles was increased to 20%. However, no further improvement in wear resistance was found as the volume fraction was increased above this level. Prasad and Calvert [17] investigated the abrasive wear behavior of composites containing quartz and glass particles in a polymethyl methacrylate (PMMA) resin. They found that particle-pull out from the matrix was the dominant wear mechanism during abrasion. In another study, McKinney [7] stated that “stress corrosion” or tribochemical reactions could play a dominant role in the wear of dental composites containing glass fillers in a polymer resin.

The composites investigated in the above mentioned studies typically contained filler particles to a maximum of about 75% by weight (or 50% by volume). More recently, composites containing higher filler contents (above 90% by weight) with superior strength and esthetics have been developed [18]. To attain higher filler content, these composites contain a percentage (5–20% by weight) of fumed silica and a broad distribution of filler particles ranging from 0.1 to 10 μm in size. This results in an efficient packing and, thus, higher strength and durability of the composites. These highly filled resin systems, which are known as “hybrid” composites, are being used as crowns or for veneering metal bridges. These are designated as “ceramic optimized polymers” or ceromers and have been suggested for use in CAD/CAM restorations. The purpose of this study is to investigate the contact wear of one of these “hybrid” ceramic dental composites, with the specific goal of determining whether the wear process in this material is controlled by microfracture or tribochemical reactions with the environment.

2. Experimental

The composite used in this study contained about 92 wt % inorganic filler particles in a polymeric resin matrix consisting of a polymerizable tetra functional monomer. According to the manufacturer [16], the resin matrix was reinforced with 16 wt % ultrafine ceramic particles (average size of 20 nm) and 76 wt % fine glass particles (average size of 1.5 μm). This composite is a commercial material (HC-ESTENIA produced by Kuraray Company, Osaka, Japan).** The exact chemical composition of the resin, the filler particles and the coupling agents were not available. The samples were light-cured and were supplied by the manufacturer in the form of disks 30 mm in diameter and 7 mm thick. Although the procedure for curing the samples could ultimately affect the properties of the composite,

no information was made available by the manufacturer on the specifics of the curing process. In order to obtain a fundamental basis for evaluating the tribological behavior of this material, a limited study was carried out to characterize the composition of the crystalline phases and filler particle size. Scanning electron microscopy (SEM), transmission electron microscopy (TEM), electron diffraction, energy dispersive x-ray analysis (EDS), and Fourier transform infrared spectroscopy (FTIR) were used. The Vicker’s hardness and fracture toughness of this material determined by indentation technique were 1.79 GPa and 1.63 $\text{MPa}\cdot\text{m}^{1/2}$ respectively [19]. The elastic modulus measured from indentation stress-strain curves and Poisson’s ratio determined by ultrasonic pulse-echo technique were reported to be 20.7 GPa and 0.26, respectively [19].

Contact wear tests were conducted using a CSEM tribometer (Geneva, Switzerland) in a ball-on-disk configuration. High-purity alumina balls (AD-995 produced by Coors, Golden, Colorado) with a hardness of 14.7 GPa were used as the counterface material due to their relatively high hardness compared to the composite. The alumina balls (12.7 mm in diameter) were used in the as received condition with a surface roughness R_a of about 0.1 μm . The composite disks were polished using diamond polishing compounds to an average surface roughness R_a of 0.1 μm . Prior to the wear tests, the alumina balls and the composite disks were rinsed with acetone and distilled water. Visual inspection and examination of the samples in SEM revealed no adverse effects (e.g., discoloration or cracking) due to the cleaning process employed in this investigation. The normal loads in the tests ranged from 1 to 20 N. The rotational speed of the disks was selected to obtain a fixed surface speed of 2.5 mm/s at the contact point between the ball and the disk. A total sliding distance of 3 m (approximately 300 rotational contact cycles) was used. Wear tests were conducted with the disks immersed in distilled water at room temperature. Based on the data reported by DeLong and Douglas [20], the total sliding distance and number of contact cycles employed in our tests simulate about 10 days of continuous wear contact in the mouth.

The friction force was monitored with a load transducer during each experiment and was recorded using a data acquisition system. Following the experiments, the average cross-sectional area of each wear track on the disk was determined from the surface profiles recorded at three different locations across the wear track using a stylus profilometer. The wear volume for each test was calculated by multiplying the average cross-sectional area of wear track by the circumference of the track. The wear tests were repeated three times at each load and the mean and standard deviation in the wear volume were calculated. The worn surfaces of the composites were examined with SEM, TEM, EDS, and micro-FTIR to assess possible changes in the chemical composition and phase structure, as well as morphological characteristics of the filler particles, in order to determine the wear mechanisms. FTIR analysis was performed directly on the sample surface in the reflection mode.

Conventional ion-beam thinning procedures were used to prepare samples from the composite for TEM

examination. In addition, a few samples were collected by gently scratching a polished surface of the composite with a diamond scribe. In order to analyze the morphology and composition of the wear debris, several samples were removed from the wear track by carefully drawing a scalpel blade along the wear track. The scratching process, in both cases, resulted in agglomerated powder rather than flakes. The powder was then deposited on a copper grid coated with a thin, "holey" carbon support film for TEM observation.

Water samples collected after the wear tests were subjected to chemical analysis to semi-quantitatively identify the possible presence of elements associated with the composite. An inductively-coupled plasma spray mass-spectrometer (ICP-MS) [21] was used for the analysis owing to its sensitivity for the detection of trace amounts (i.e., few ng/ml) of various elements in solution. Water samples were placed in closed glassware for several days to allow precipitation of the wear debris before analysis by ICP-MS. Prior to the analysis of used water samples, a sample of distilled water also stored in a glass vial was analyzed as the reference. In order to confirm the results of chemical analysis, the water after one wear test was stored in a polyethylene bottle instead of a glass vial. In addition, water sample was collected after a static immersion test in which the composite sample was set up in the tribometer in exactly the same manner as it would have been done for a wear test, but without making a contact with the alumina counterface. The composite sample was rotated at the same speed used during the wear tests. The water sample was then stored in a polyethylene bottle for subsequent chemical analysis.

3. Results

3.1. Characterization of the composite

SEM examination of polished surfaces of the composite typically revealed a fully dense structure containing a uniform distribution of filler particles of varying sizes, Fig. 1. Based on these observations, the size of the filler particles range from about 0.5 to 10 μm . TEM examination of ion-thinned samples revealed a similar

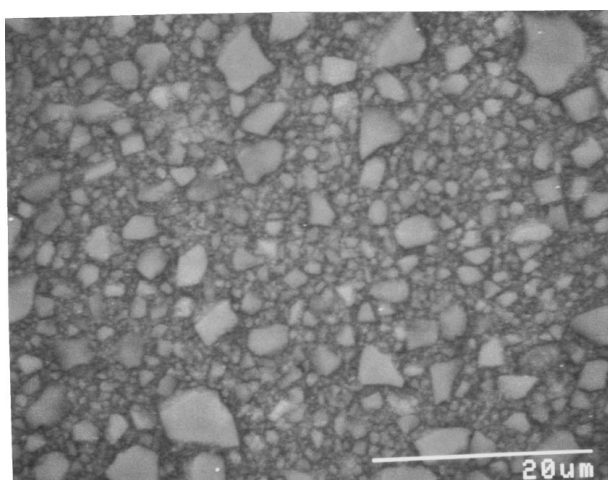


Figure 1 SEM micrograph of the polished surface of the composite, showing filler particles of various sizes.

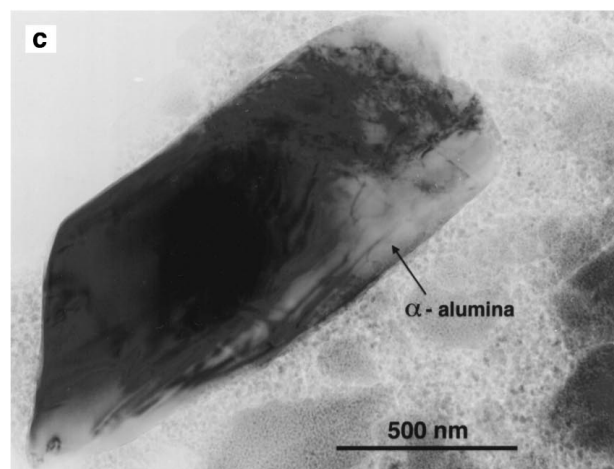
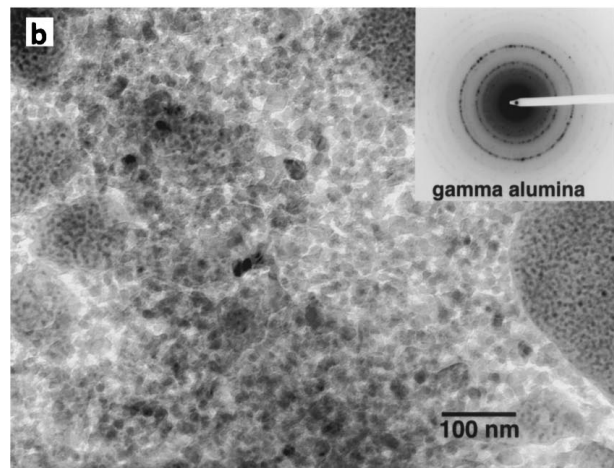
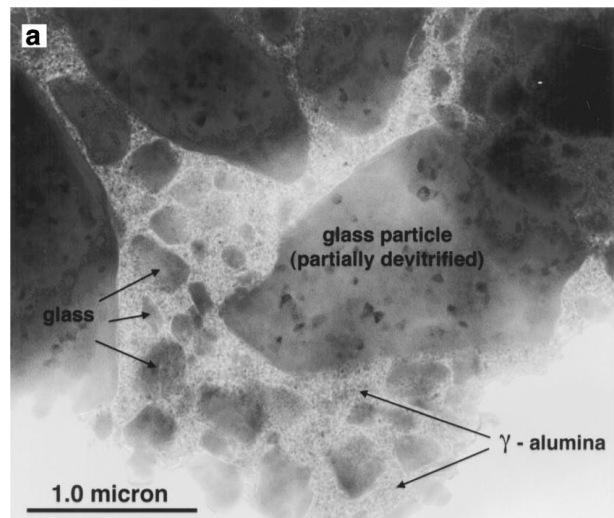


Figure 2 (a) TEM micrograph of the ion-thinned specimen showing (a) large glass particles, (b) fine (20 nm) filler particles [inset: electron diffraction pattern corresponding to gamma- Al_2O_3], and (c) large alpha- Al_2O_3 particle.

distribution of filler particles, as well as other details of the microstructure. From Fig. 2a, for example, it can be seen that the large filler particles ($>1.0 \mu\text{m}$ in size) are distributed within a matrix of much smaller particles, all being held together by the polymeric resin. The larger filler particles can be identified as a glass, which contains nano-scale crystallites due, presumably, to partial devitrification of the glass phase. Without regard to

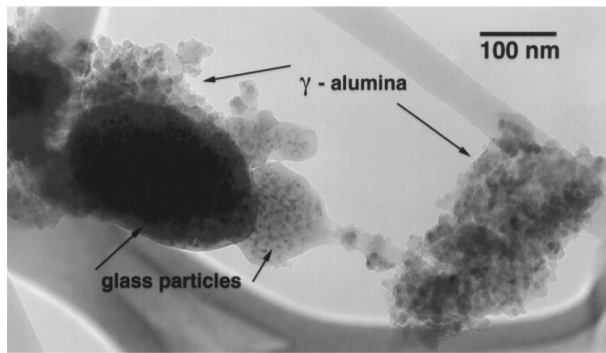


Figure 3 TEM micrograph of the particles removed by scratching the composite indicating a mixture of nano-scale gamma-Al₂O₃ particles and glass particles similar to Fig. 2.

these crystalline products of devitrification (which typically decompose on exposure to the electron beam), electron diffraction and energy dispersive x-ray analysis (EDS) indicated that the large filler particles can be qualitatively described as an alumino-silicate glass containing lanthia and zirconia as major additive constituents. Between the large glass filler particles, the matrix was found to consist of similar, but smaller (down to 100 nm), glass particles and a relatively dense agglomerate of 20–30 nm size gamma-Al₂O₃ particles, Fig. 2b. Here, gamma-Al₂O₃ was readily identified from selected area electron diffraction (inset Fig. 2b) and EDS. In addition, several alpha-Al₂O₃ particles (typically 1–30 μm in size) distributed within the composite were readily identified by electron diffraction and EDS, Fig. 2c.

The results obtained on the ion-thinned samples were compared with particulate obtained by gently scratching a polished surface of the composite with a diamond scribe. As illustrated in Fig. 3, the particles produced by scratching also can be described as a mixture of nano-scale gamma-Al₂O₃ particles and larger glass particles, whose physical and chemical attributes are identical with those determined from observations on ion-thinned samples. These particles show no evidence for microstructural changes due to scratching or exposure to the environment and, thus, provide a more direct basis for comparison with the particulate obtained from the wear tracks.

3.2. Wear volume and friction coefficient

Typical surface profiles recorded across the wear tracks of the composite samples tested at two different loads are shown in Fig. 4. The maximum depth of the wear track in this example, is about 1.5 μm at the low load (1 N) and 3.5 μm at the higher load (15 N). The widths of the wear tracks are 100 and 200 μm, respectively. The measured wear volumes are plotted as a function of load in Fig. 5. The wear volume slightly increases as the load is increased from 1 to 5 N. As the load is further increased to 10 N, the wear volume increases by one order of magnitude. At loads above 10 N, the wear volume is independent of load. As expected, examination of the alumina counterface in the SEM showed no evidence for significant wear at any of the loads used in this investigation.

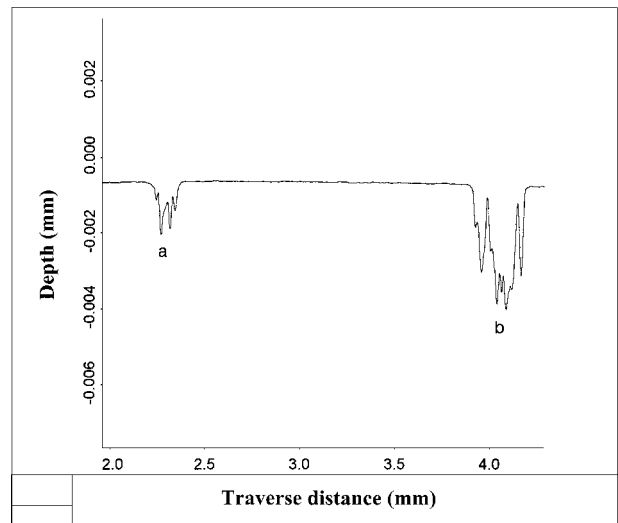


Figure 4 Typical surface profile traces of the wear track at (a) 1 N and (b) 15 N.

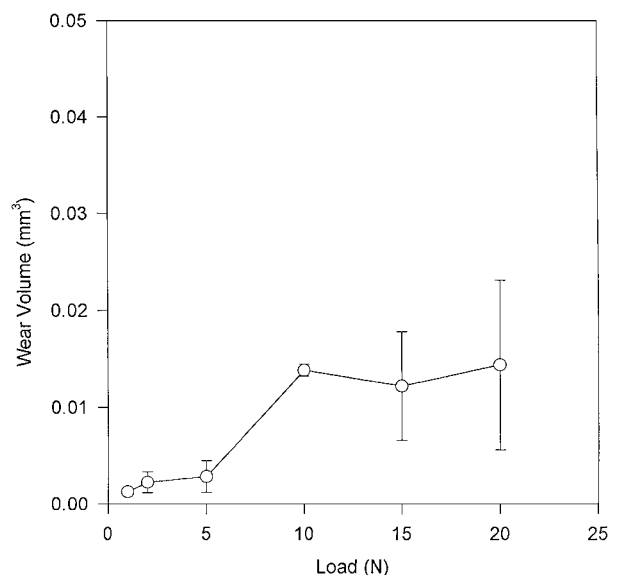


Figure 5 Wear volume of the composite as a function of load, revealing two wear regimes. The data points correspond to the mean values and the uncertainty bars indicate ± one standard deviation.

Typical friction force traces at loads of 1 and 15 N are shown in Fig. 6. At the low load, the friction force quickly attains a steady state value and remains in that state until the end of the test. The variations in the force signal at the low load are small. During the high load test, the friction force signal is erratic and does not attain a steady state condition during the testing period. The coefficients of friction calculated from the friction force traces for the last 10 min of sliding (out of 20 min total test duration) as a function of load are shown in Fig. 7. Note that the mean coefficient of friction decreases from about 0.71 to 0.43 as the load is increased. The uncertainty bars in the plot designate ± one standard deviation for the repeat measurements, and not the variation in the signal during the tests.

3.3. Characterization of the wear tracks

As a first step in investigating the reasons for the change in wear behavior with load, the wear tracks were

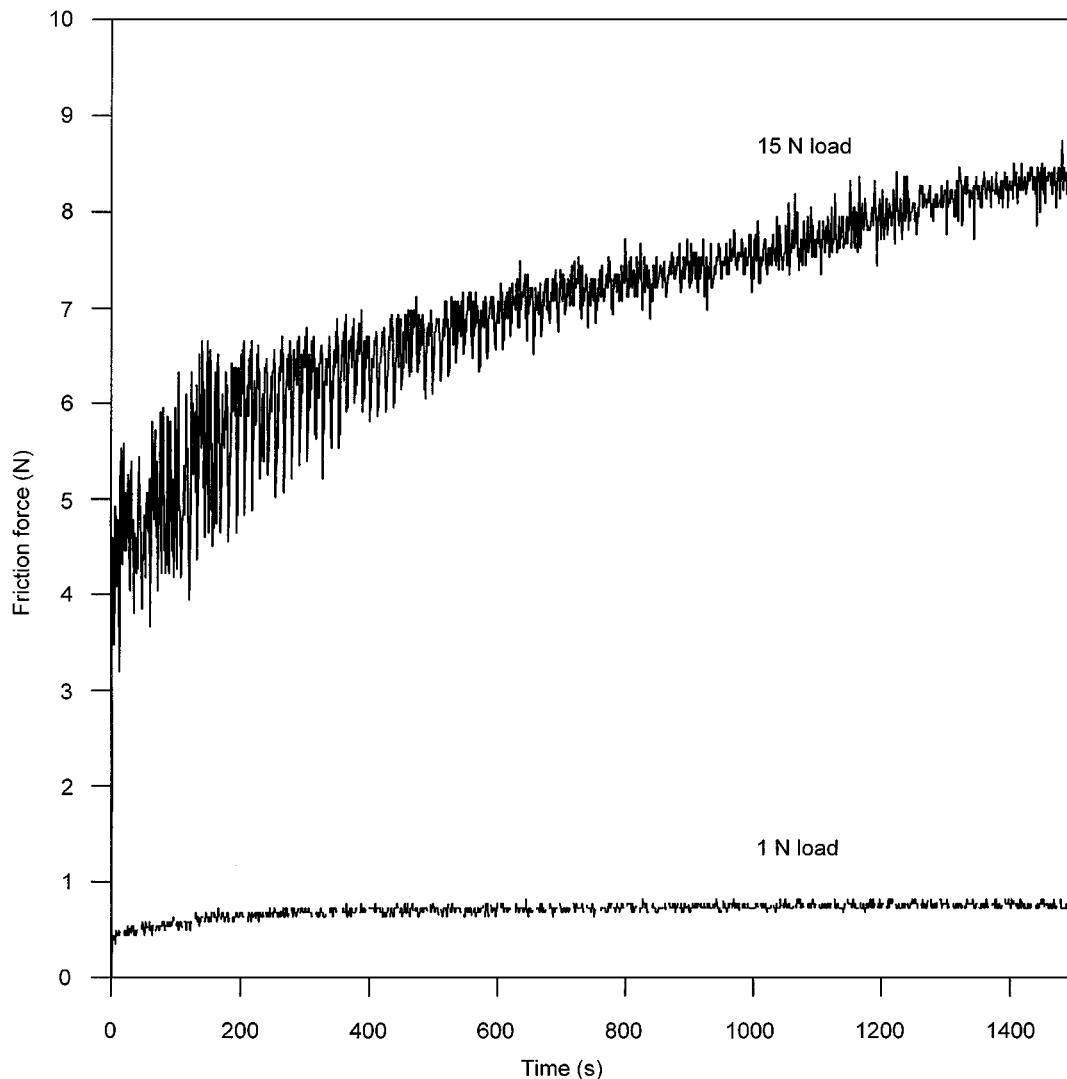


Figure 6 Typical friction force traces at a low load (1 N) and a high load (15 N).

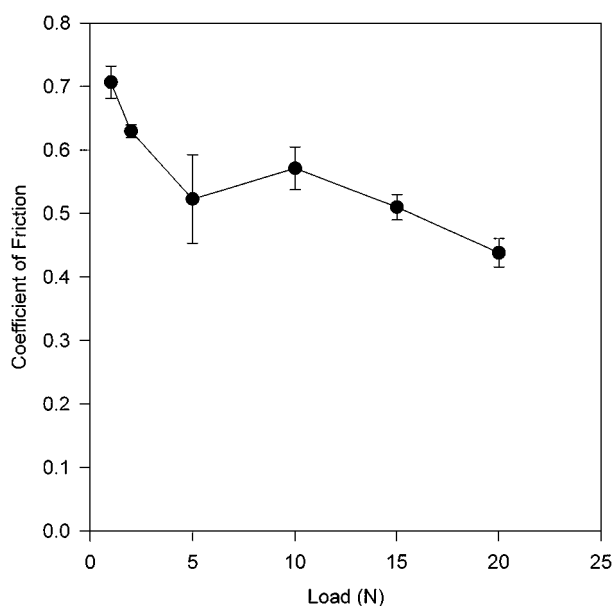
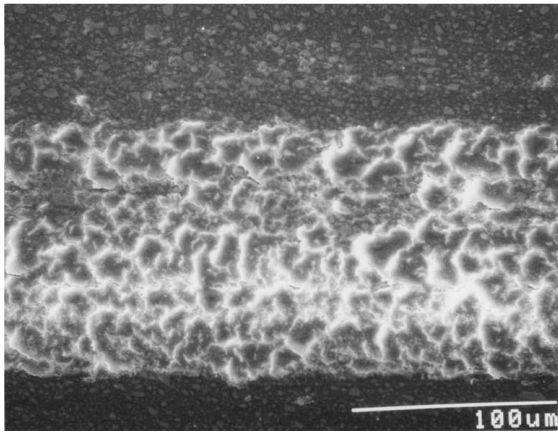


Figure 7 Average coefficient of friction as a function of load.

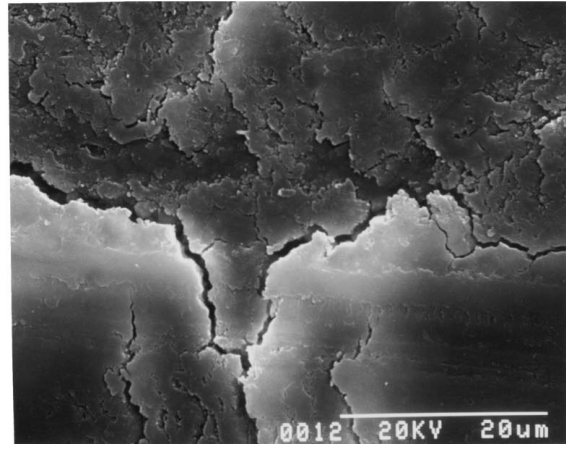
examined by SEM. A low magnification micrograph typical of the wear tracks at low loads is shown in Fig. 8a. In this micrograph the wear track is delineated by an adhered surface film, which exhibits bright con-

trast relative to the background polished surface. At higher magnifications, Fig. 8b, the film is seen to have a relatively smooth surface and to contain numerous microcracks. To determine whether these microcracks formed during water lubricated sliding or as a result of subsequent drying, the wear track of a repeat test was examined by optical microscopy immediately after the wear test. The observations revealed relatively few microcracks within the wear track. This sample was then dried in an oven at 150 °C for 30 min. Re-examination by optical microscopy revealed a significant increase in the number of microcracks within the wear track after drying. This experiment suggests that although microcracks can form during the wear test, most of the microcracks observed in the SEM form as a result of dehydration of the surface film.

SEM examination of wear track films formed at higher loads, Fig. 9a, revealed morphological features similar to those found at the low loads. However, partial detachment of the surface film from the wear track was also observed. Within the regions where film detachment is observed, Fig. 9b, the structure of the glass filler particles and pits due to particle pull-out can be seen. In addition, the surface film, seen in the upper left corner of this micrograph, is found to be composed of an aggregate of fine particles.

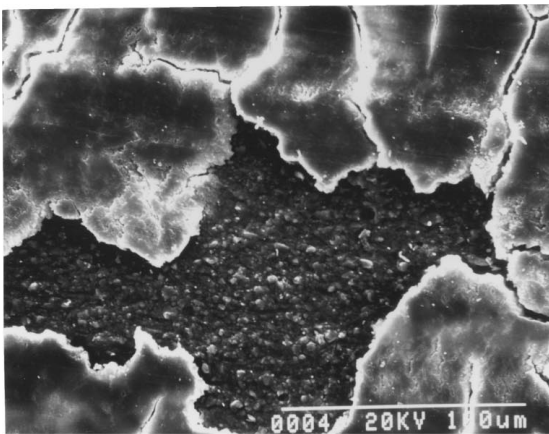


(a)



(b)

Figure 8 Typical SEM micrograph of a wear track on the composite at 1 N showing (a) a surface film at low magnification and (b) “mud-cracks” at high magnification.

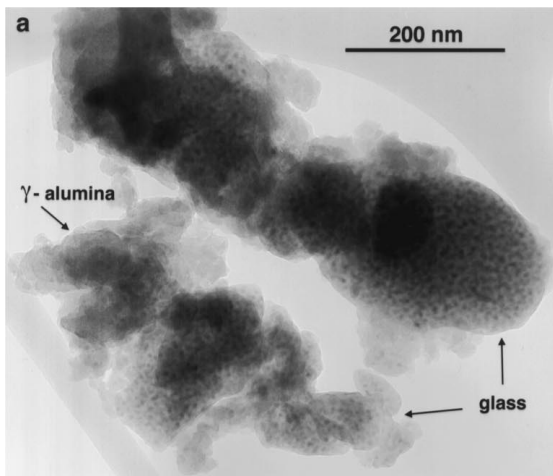


(a)

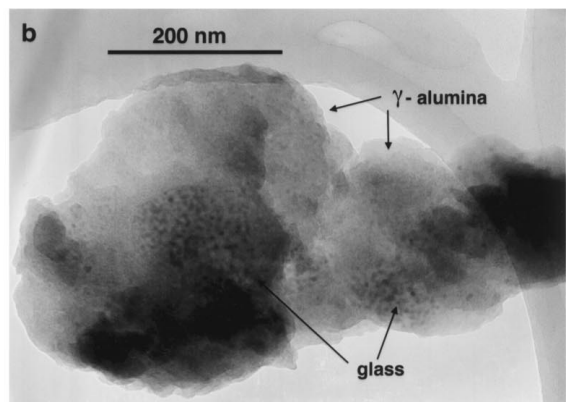


(b)

Figure 9 SEM micrograph of the wear track at 15 N showing (a) the detachment of the surface film and (b) detached locations revealing particle pull-out from the resin matrix and fragmented particles.



(a)



(b)

Figure 10 (a) TEM micrograph of the surface film revealing fine crystalline particles of alumina and glass particles (a) at 1 N, and (b) at 15 N.

To further investigate the nature of the adhered films on the wear tracks, portions of the films produced during a low load and a high load wear test were removed from the wear tracks for examination by TEM. Selected, but characteristic, aggregates of particles ob-

tained from these films are shown in Fig. 10a and b. Irrespective of the test load, the wear film aggregates can be described as a mixture of nano meter-scale (20–30 nm) gamma- Al_2O_3 crystallite particles and smooth, but irregularly shaped glass particles of varying sizes.

No differences could be found in comparing electron diffraction or EDS results from the crystalline and glass phases present in both sets of wear track films. Moreover, these results are consistent with those obtained from polished unworn regions (Figs 2 and 3), discussed earlier. Because TEM examination was restricted, not only to a small volume of wear track film but to particle clusters sufficiently thin to be transparent to electrons, no comparison of the size distribution of discrete particles contained within the wear track films and those present in the unworn material could be made. While, there was no evidence suggesting that the glass particles in the wear track film were formed as a result of fracture of the large glass particles that were present in the composite material, this possibility can not be discounted. In addition, no evidence of $\alpha\text{-Al}_2\text{O}_3$ particles was found in the wear track films, despite their presence in the composite material. This observation is also consistent with the no-wear condition of the alumina counterface since the counterface material was primarily made from alpha-alumina.

Comparison of particulate from the wear track, Fig. 10, with those removed by scratching from a polished surface, Fig. 3, reveals a small, but apparent difference in the image contrast exhibited by the individual $\gamma\text{-Al}_2\text{O}_3$ particles. Specifically, the individual gamma-phase particles were invariably more sharply defined within the clusters of particles produced by scratching, Fig. 3, than those found within clusters of

particles obtained from wear track films, Fig. 10. In fact, examination of the film particles often required the use of electron diffraction and/or dark field imaging to verify the presence of $\gamma\text{-Al}_2\text{O}_3$ particles in regions that otherwise exhibited apparent amorphous contrast. While this difference in the appearance of the $\gamma\text{-Al}_2\text{O}_3$ crystallites suggests changes in either the surface structure of the crystallites or changes in the substance that surrounds and binds the crystallites together, definitive evidence for either of these changes could not be obtained. Thus, while we cannot specify the reason for this observed difference in image contrast, it is reasonable to assume that it was brought about by the wear process.

The FTIR spectra typical of the surface films on the wear tracks at a low load (1 N) and a high load (15 N) are shown in Fig. 11a and b, respectively. The background spectrum, Fig. 11c, obtained from an unworn region on the sample is also shown in the figure for comparison. This spectrum shows major peaks at 700, 950, 1050, and 1680 cm^{-1} . Note that the sharp valley at about 1250 cm^{-1} in the spectra is due to reflection from the surface and is not associated with chemical bonds. The spectra for the two wear tracks obtained at the two different loads are essentially identical, but in comparison with the background spectrum, three new peaks are identified. The additional peaks observed on the surface film are attributed to $\text{Al}(\text{OH})_3$ (at 764 and 3600 cm^{-1}) and hydrated silica (at 1180 and

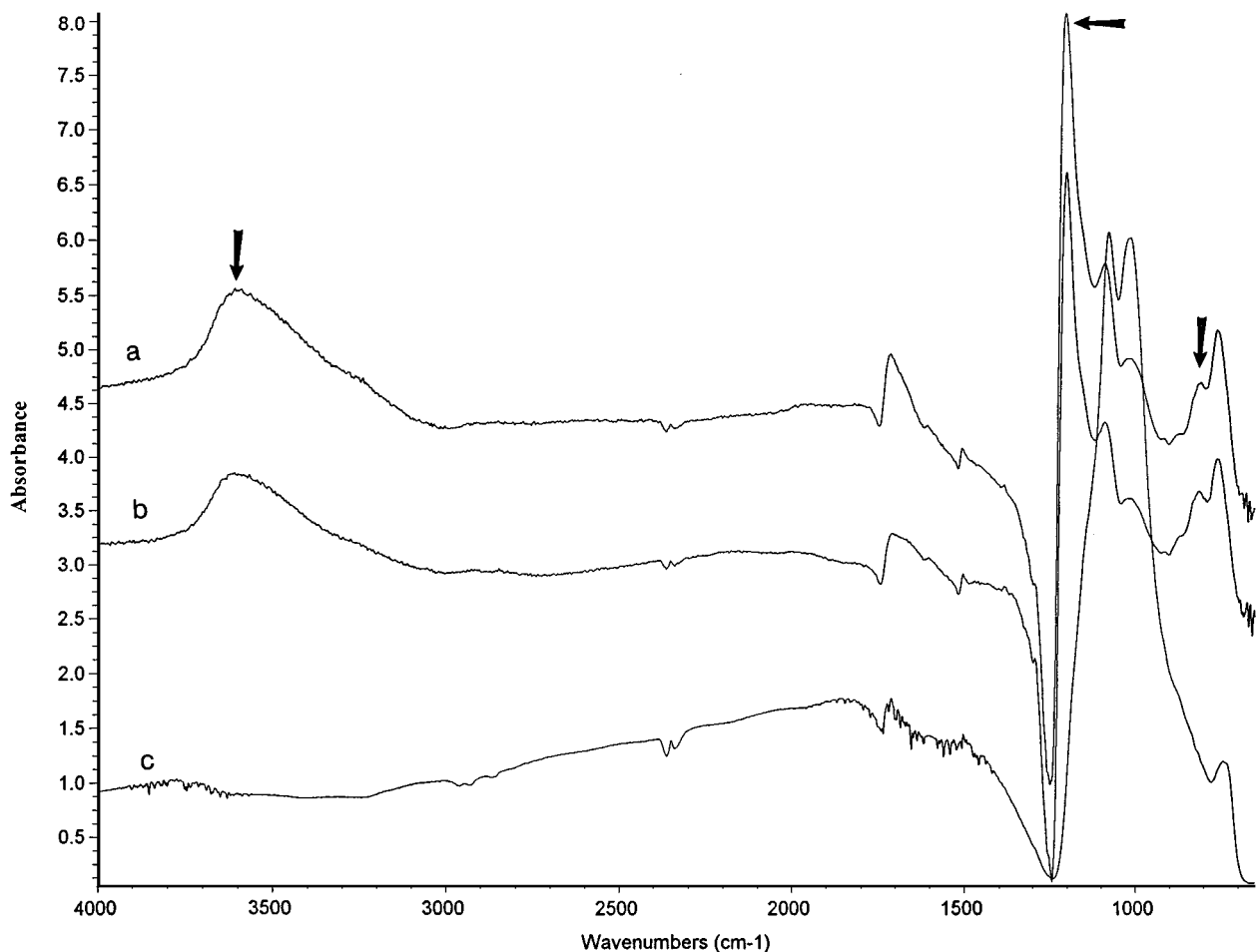


Figure 11 FTIR spectra of (a) the surface film at 1 N, (b) surface film 15 N, and (c) unworn surface. Additional bands (indicated by arrows) observed on the surface film are attributed to $\text{Al}(\text{OH})_3$ and $\text{SiO}_2 \cdot x\text{H}_2\text{O}$.

3600 cm^{-1}). This observation is in agreement with earlier FTIR reports of Van der Marel and Beutelspacher [22] for $\text{Al}(\text{OH})_3$ and FTIR studies of Enomoto and Mizuhara [23] on silica gel. The appearance of a band at 3600 cm^{-1} due to hydroxyl group in the surface film suggests an enhanced reaction of silica-rich glass particles and alumina filler particles with water during sliding. Since tribochemical reactions often produce amorphous products [24], some of the amorphous material observed by TEM in the surface films extracted from the wear tracks is likely to be aluminum hydroxide and hydrated silica identified by FTIR.

3.4. Chemical analysis of distilled water

In a purely tribochemical wear process [25], removal of the surface films occurs by dissolution of the reacted products (e.g., aluminum hydroxide and hydrated silica) in water. In order to examine this possibility, water samples collected after the wear tests were subjected to chemical analysis by an inductively-coupled plasma spray mass-spectrometer (ICP-MS) to identify the possible presence of Al and Si in water. Water samples that were placed in closed glassware for several days to allow precipitation of the wear debris were visually inspected. For low load tests, the water samples were clear both before and after storage with no visible debris. However, the water samples were cloudy after the wear tests performed at high loads, and became clear after storage. Two water samples collected at two different loads representing a low load and a high load test were analyzed plus an unused distilled water sample for baseline comparison. Following the analysis, the spectrum for baseline water was subtracted from the spectra of the used water samples. Similar analysis was conducted on two water samples that were stored in polyethylene bottles, one collected from a repeat wear test at 15 N and the other from the static immersion test. It should be noted that the uncertainty associated with the elemental concentration obtained in this analysis is about $\pm 20\%$. While the unused water sample did not show any major impurities, the used water samples stored in glass bottles had an abundant amount of Si; but those stored in the polyethylene bottles had a much lower Si content. However, because of possible interference between the signals for Si and N, it is doubtful whether the Si results are significant. The results for the static immersion test in Table I indicate that small amounts of Li, Ba, and La have been dissolved in the

water solution. However, no Al, Zr, or Ta was found in the water solution after the static immersion test. While there was no significant difference in the concentration of various elements detected in the water samples stored in the two different containers, the results obtained from the static test and the wear tests are different. There is also a significant increase in the concentration of some of the elements, for example Li and Al, as the load used in the wear test is increased. In comparison with static immersion, the results indicate that the concentration of Li, Al, La, Ta, and Zr have increased as a result of wear testing. The Ba concentration detected in water after the static immersion test and the wear test are not significantly different. Although such elements as Li, Al, Ba, La, and Zr are associated with the filler particles in the composite investigated in the present study, the source of Ta is not known.

4. Discussion

The results on wear volume of the hybrid ceramic composite indicate that the wear process in this material depends on the load employed during the test. The wear volume is small at low loads, but increases by one order of magnitude when the load is increased from 5 to 10 N. Such a drastic increase in the wear volume suggests a change (or a transition) in the wear mechanism [26]. Examination of the worn surfaces indicated that a thin film was present in the wear track, irrespective of the load. While at low loads, the wear track was completely covered, the film was discontinuous at high loads and was partially removed. The wear film was found to be composed of a mixture of gamma- Al_2O_3 crystallites and glass particles, both from the substrate. Since no difference in the structure and composition of the wear films were found as a function of load, it is hypothesized that the large increase in the wear volume is due to film detachment at the higher loads. However, wear becomes independent of load at high loads, despite the fact that wear is dominated by mechanical detachment of the surface film.

Analyses by SEM and TEM indicated that the microstructure of the hybrid ceramic composite consists of large (1–10 μm) particles of alumino silicate glass in a matrix containing smaller glass particles and gamma- Al_2O_3 particles. In addition, isolated alpha- Al_2O_3 particles were occasionally found dispersed within this composite. The nano meter-scale gamma- Al_2O_3 particles were also observed in the particulate collected from the wear films. These films also contained sub-micro meter glass particles from the substrate material or resulting from fracture of the glass particles found in the substrate. The TEM results suggested a change, as a result of wear, in either the surface structure of the gamma- Al_2O_3 particles or the matrix that surrounded these particles. These observations together with the FTIR results suggest that the silica glass and alumina filler particles had reacted on the wear track with water forming hydroxides and hydrated compounds of silicon and aluminum. Considering the large amount and the small size of gamma- Al_2O_3 particles, as compared to the much larger alpha- Al_2O_3 particles, and the TEM

TABLE I Concentration of elements present in the water samples as obtained by ICP-MS

Elements	Concentration after static immersion (ng/ml)	Concentration after wear test at 2 N (ng/ml)	Concentration after wear test at 15 N (ng/ml)
Li	2.8	8.2–8.6	20–71
Al	0	9–12	12–17
Ba	0.3	0.35–0.40	0.08–0.75
La	0.3	0.88–0.89	0.95–9.16
Ta	0	0.26–0.28	0.28–0.93
Zr	0	0.78–0.88	0.37–0.47

results on the structural change in the gamma-alumina particles, it is suggested that the hydrated alumina products observed in the surface film are associated with the gamma-alumina due to its high reactivity associated with the larger surface area.

These observations suggest that the wear film is composed of a mixture of reaction products and fragments from the base composite (i.e., polymeric resin and small gamma-Al₂O₃ crystallites). We hypothesize that the fragments from the substrate material are removed by a small-scale fracture process and that the shearing action associated with sliding at the contact mixes the hydrated reaction products with the fragments. Although, the tribochemical reactions occur more readily at the contact between the counterface and the wear film because of the higher temperatures at the intimate contact region, water can also diffuse along the microcracks in the film and react with the particles in the substrate. The rate of film formation is expected to increase with load, because of the dependence of contact temperature on load, as well as an increase in the supply of substrate fragments to the film as the load is increased.

The tribochemical reactions (i.e., formation of hydrated oxides on the wear track) can be rationalized based on the chemical affinity of silica and alumina with water. Formation of hydroxides on silicon nitride [24–26], silicon [27] and alumina [28–30] during wear have been reported in the literature. Gates *et al.* [28] attributed the tribochemical reactions between alumina and water to the formation of reactive transient phases, such as bayerite. Dong *et al.* [29] and Jahanmir and Dong [30] observed that formation of aluminum hydroxide phases dominated the friction and wear behavior of alumina.

Since the wear film consists of loosely held aggregates of crystalline and amorphous particulates, some of the particles or agglomerates may be removed by mechanical means, for example, the shearing action at the sliding interface and microfracture. The rate of film removal by fracture is expected to increase as the load is increased. However, film failure and local detachment occur either at a critical load, or as the film thickness reaches a critical thickness (which also depends on the load), resulting in a large increase in the wear volume or a wear transition.

Contact wear can also occur by tribochemical means, i.e., removal through dissolution of the reaction products in water [25]. As hydrated oxides of Si and Al can readily dissolve in water, it is not surprising to find elemental Al (from aluminum oxide particles), and Li, La, and Zr (from the glass particles) in the water solution after the wear tests. However, one cannot rule out the possibility for the presence of small nanometer sized particles in solution during chemical analysis. Although the water samples did not contain any visible wear debris and the large particles were removed by the aerosol filters just prior to ICP analysis, the water samples collected after the wear tests could have contained small nanometer sized wear debris.

The results of this study suggest that the hybrid ceramic composite evaluated in this investigation is subjected to a complex set of processes at the contact

which include tribochemical reactions, dissolution, and mechanical removal. The observed load-independent wear behavior at high loads requires further explanation, since material removal by mechanical action alone should be load-dependant. We hypothesize that this behavior may be related to a combination of tribochemical and mechanical processes. For wear by mechanical process [31, 32], the wear rate or the rate of reduction in film thickness is proportional to load L such that

$$dx/dt \propto L^n \quad (1)$$

where n is usually about 1. However, the rate of film formation by tribochemical reactions is related to the contact temperature [31, 32], which is related to the load, i.e.,

$$dx/dt \propto \text{Exp}(-Q/RT) \quad (2)$$

where Q is the activation energy for reaction, R is the gas constant, and the contact temperature T is

$$T \propto fVL$$

where f is the coefficient of friction and V is the surface speed. For dissolution, similar to other thermally activated processes,

$$dx/dt \propto \text{Exp}(-Q/RT) \quad (3)$$

All three processes of film formation, dissolution, and fracture can occur simultaneously. It may be noted that at high loads, the rate of film growth may be large enough to compensate for dissolution or increase in mechanical wear; thus, resulting in a load-independent behavior.

Since both tribochemical reactions and microfracture are important processes in determining the wear rate of the hybrid ceramic composite studied in the present investigation, the wear behavior of this composite could be altered by changes in the chemical composition of the filler particles as well as particle size and distribution. The role of resin matrix in the tribochemical reaction and film formation needs to be investigated further, since water aging of the composites could result in differences in mechanical properties of this type of composite [33]. It should be noted that the present investigation was carried out to assess the fundamental contact wear processes on the hybrid ceramic composite. Therefore, no attempt was made to assess the clinical relevance of the results presented in this paper. This could be the subject of a future investigation.

5. Conclusions

Contact wear of the studied composite (HC-ESTENIA) is controlled by three simultaneous wear processes, viz., tribochemical reactions and film formation, dissolution of tribochemical products in water, and mechanical removal of the film by microfracture. At low loads, wear is dominated by the tribochemical mechanisms; whereas at high loads wear occurs by a combination of

tribochemical mechanisms and detachment of the surface film. Our results indicate that optimization of the wear behavior of this composite may require a change in the chemistry as well as the size distribution of the filler particles.

Acknowledgements

We thank Sinichi Sato of Kuraray Co., for providing the composite material for this study. We acknowledge the assistance received from Lewis Ives, Joseph Ritter, Greg Turk, Richard Gates, Lee Yu, and Frank Yin of NIST in chemical analysis. We also thank Dianne Rekow of UMDNJ for discussions and overall guidance. This project was funded by NIH-NIDCR under a contract to the University of Medicine and Dentistry of New Jersey (Contract # 1 P01DE10976-01A1).

References

1. M. Z. A. M. SULONG and R. A. AZIS, *J. Prosthet. Dent.* **63** (1990) 342.
2. L. M. MAIR, *J. Dent.* **20** (1992) 140–144.
3. D. G. GROSSMAN, in "Int. Symp. on Computer Restorations: State of the Art of the CEREC-Method," edited by W. H. Moremann (Quintessence, Chicago, IL, 1991) p. 103.
4. R. DELONG, C. SASIK, M. R. PINTADO and W. H. DOUGLAS, *Dent. Mater.* **5** (1989) 266.
5. D. W. JONES, in "Encyclopedic Handbook of Biomaterials and Bioengineering," edited by D. L. Wise, D. J. Trantolo, D. E. Altobelli, M. J. Yazemski, J. D. Gresser and E. R. Schwartz (Marcel Dekker, New York, 1995) p. 141.
6. V. S. NAGARAJAN and S. JAHANMIR, *Wear* **200** (1996) 176.
7. J. E. MCKINNEY, in "International Symposium on Posterior Composite Resin Dental Restorative Materials," edited by G. Vanherle and D. C. Smith (1985) p. 331.
8. G. WILLEMS, P. LAMBRECHTS, M. BRAEM and G. VANHERLE, *Quintessence Int.* **24** (1993) 641.
9. T. J. BLOEM, G. C. MCDOWELL, B. R. LANG and J. M. POWERS, *J. Prosth. Dent.* **60** (1988) 242.
10. J. R. CONDON and J. L. FERRACANE, *Dent. Mater.* **12** (1996) 218.
11. W. W. JOHNSON, V. B. DHURU and W. A. BRANTLEY, *ibid.* **9** (1993) 95.
12. A. HTANG, M. OHSAWA and H. MATSUMOTO, *ibid.* **11** (1995) 7.
13. J. M. POWERS and S. C. BAYNE, "ASM Handbook Volume 18" (ASM International, USA, 1992) p. 665.
14. S. SUZUKI, J. W. OSBORNE and K. F. LEINFELDER, *J. Esth. Dent.* **8** (1996) 263–268.
15. S. W. HAN and T. A. BLANCHET, *ASME J. Tribol.* **119** (1997), 694.
16. J. M. DURAND, M. VARDAMOULIAS and M. JEANDIN, *Wear* **181–183** (1995) 833.
17. S. V. PRASAD and P. D. CALVERT, *J. Mater. Sci.* **15** (1980) 1746.
18. K. OKADA, I. OMURA and J. YAMAUCHI, *J. Dent. Res.* **76** (IADR Abstracts) (1997) p. 195.
19. S. LIKITVANICHKUL and B. R. LAWN, (1997), unpublished results.
20. R. DELONG and W. H. DOUGLAS, *IEEE Trans. Biomedical Eng.* **38** (4) (1991) 339.
21. G. HORLICK, *Spectroscopy*, **7**(1) (1992) 22.
22. H. W. VAN DER MAREL and H. BEUTELSPACHER, "Atlas of Infrared Spectroscopy of Clay Minerals and their Admixtures" (Elsevier Scientific Publishing Company, New York, 1976) p. 192.
23. Y. ENOMOTO and K. MIZUHARA, *Wear* **162–164** (1993) 119.
24. T. E. FISCHER and H. TOMIZAWA, *ibid.* **105** (1985) 29.
25. S. JAHANMIR and T. E. FISCHER, *Tribol. Trans.* **32** (1989) 32.
26. X. DONG and S. JAHANMIR, *Wear* **165** (1993) 169.
27. K. MIZHURA and S. M. HSU, in "Wear Particles," edited by D. Dowson (Elsevier, New York, 1992) p. 323.
28. R. S. GATES, S. M. HSU and E. E. KLAUS, *STLE Tribol. Transc.* **32** (1989) 357.
29. X. DONG, S. JAHANMIR and S. M. HSU, *J. Amer. Ceram. Soc.* **74** (1991) 1036.
30. S. JAHANMIR and X. DONG, in "Friction and Wear of Ceramics," edited by S. Jahanmir (Marcel Dekker, New York, 1994) p. 15.
31. T. F. J. QUINN and J. L. SULLIVAN, *NASA Report NCC-3-14* (1982) 110.
32. T. F. J. QUINN, *Tribol. Intl.* **16** (1983) 305.
33. D. J. INDRANI, W. D. COOK, F. TELEVANTOS, M. J. TYAS and J. K. HARCOURT, *Dent. Mater.* **11** (1995) 201.

Received 6 October 1997
and accepted 21 June 1999